POLYMORPHISM

The genetics, evolution, and maintenance of a biological rock-paper-scissors game

Ammon Corl[1,2]*, Alex Guzman[1,2], Ke Bi[1,2], Juan Manual Vazquez[2], Lydia L. Smith[1,2], Pauline Blaimont[3,4], Regina Spranger[3,5], Robert D. Cooper[6], Donald Miles[7], Amy Goldberg[8], Jian Gao[9], Xueyan Xiang[10,11], Yang Zhou[11], Qiye Li[9,10,11], Guojie Zhang[12], Peter H. Sudmant[2], Rauri C. K. Bowie[1,2], Jimmy A. McGuire[1,2], Barry Sinervo[3]†, Rasmus Nielsen[2,13,14]

Side-blotched lizards (*Uta stansburiana*) play a biological rock-paper-scissors game in which three differently colored male morphs utilize alternative mating strategies. We identified the genetic basis of this polymorphism, which was previously posited to arise from three alleles at one locus. Orange usurper and blue mate-guarder morphs are associated with two divergent haplotypes in the regulatory region of the sepiapterin reductase gene, but yellow sneaker morphs appear to arise through phenotypic plasticity from the same genetic background as blue morphs. Our simulations show that rock-paper-scissors dynamics can better maintain a polymorphism with a genetic system of two alleles plus plasticity than with a three-allele system. This form of balancing selection that combines genetic determination with phenotypic plasticity expands the possibilities for how stable polymorphisms arise in nature.

Phenotypic differences within species allow adaption to novel environments and the formation of new species, so it is important to understand the factors that generate and maintain this variability (*1*–*5*). Species can exhibit distinct morphs that differ across multiple traits, such as coloration and behavior (*2*, *6*–*11*). Understanding how morphs coexist within a population can reveal the selective forces that maintain variation within species (*6*, *12*, *13*). Balancing selection on morphs has been investigated for decades in a population of side-blotched lizards (*Uta stansburiana*) where three color morphs are observed, each associated with a distinct male mating strategy (Fig. 1A and fig. S1). The competitive dynamics among these morphs were the first known example of a biological rock-paper-scissors game (*6*). Orange-throated males can dominate blue males and control large territories with many females because of their greater testosterone levels and endurance (*14*, *15*). Blue-throated males guard females to reduce extrapair paternity, giving them an advantage over yellow-throated males that obtain most of their reproductive success through extrapair matings (*15*). Yellow-throated males do not defend a territory but rather sneak onto other males' territories to obtain mates, which works well in the large territories of orange males (*6*, *15*). Each morph has high fitness when one competitor morph is common and low fitness when the third competitor is common, and morph frequencies cycle over time (*6*, *16*, *17*). Research on side-blotched lizards has been influential for understanding how polymorphic strategies are maintained (*6*, *17*–*19*) and how morphs can differ across a suite of traits including coloration, behavior, hormone levels, and brain morphology (*6*, *14*, *15*, *20*–*22*).

Genetic studies of polymorphic species have revealed much about the development of their complex phenotypes and how multiple traits such as coloration and behavior can vary together (*7*–*11*, *23*). Morphs often arise from a "supergene" in which genetic differences across multiple genes are linked as a result of suppressed recombination, typically through a chromosomal inversion (*7*, *9*, *10*, *23*). However, other genetic mechanisms could give rise to complex morph phenotypes, such as a single pleiotropic gene that affects multiple traits (*11*, *24*) or two unlinked loci that affect different morph phenotypes (*8*). In addition, phenotypic plasticity can generate differences in morphology and behavior similar to those observed among genetically determined morphs (*1*, *4*, *25*–*28*) and can affect how morphs are maintained in a population (*1*, *28*). Therefore, the role and interaction of genetic and environmental factors needs to be determined to understand how polymorphic phenotypes develop.

In this study, we investigated the genetic basis of the color morphs observed in side-blotched lizards to understand how they develop and how the rock-paper-scissors system evolved. Determining the genetic basis of the polymorphism is also critical for clarifying how it is maintained, because the evolutionary dynamics of the morphs have typically been modeled with their phenotypes arising from a single locus with three alleles (*29*). This three-allele model has been the foundation for decades of field and theoretical studies on *U. stansburiana* (*6*, *16*, *17*, *30*, *31*). Although some heritability of coloration has been observed (*30*, *31*), the genetic basis of the color polymorphism has remained unresolved (*29*). Below, we determine the genetic system underlying the color morphs and update the models describing their evolutionary dynamics.

Results

The three morphs exhibited distinct throat colors (Fig. 1A and fig. S1). The orange and yellow colors likely arise from pigments, whereas the blue is likely structural coloration (*8*, *20*, *32*, *33*). We first investigated the genetics of the orange and blue morphs, because they had the most distinctive color phenotypes (fig. S1, E and F) and potentially different mechanisms generating their coloration.

We assembled two genomes, one for an orange morph and one for a blue morph. We then performed a genome-wide association study with 44 orange morphs and 45 blue morphs chosen from a single population for their distinctive phenotypes. No genome-wide differentiation was detected between the morphs (fig. S2). Instead, a single genetic region was highly associated with the orange versus blue morph phenotype for both reference genomes (Fig. 1B and figs. S3, A and B, and S4, A and B). The strongest associations [minimum *P* value (P_{min}) = 7×10^{-19}] were located upstream of the gene for sepiapterin reductase (*SPR*). Only weak associations were observed in the *SPR* coding region ($P_{min} = 0.003$) (*29*). The *SPR* gene is involved in two pathways relevant to the morph phenotypes (fig. S5). First, *SPR* helps synthesize tetrahydrobiopterin, which is an essential cofactor for the enzymes that synthesize dopamine, adrenaline, noradrenaline, melatonin, and serotonin (*34*, *35*). Second, *SPR* is part of the pathway for synthesizing pteridine pigments (*36*), and an orange drosopterin pteridine pigment has been found in throat skin of orange morphs but not in blue morphs (*20*). Also, structural variation upstream of *SPR* was associated with orange and white morphs in the distantly related European common wall lizard (*Podarcis muralis*) (*8*). The dual role of *SPR* could therefore allow a color signal to be coupled with differences in hormones or neurotransmitter levels that affect behavior (fig. S5) (*29*).

[1]Museum of Vertebrate Zoology, University of California, Berkeley, Berkeley, CA, USA. [2]Department of Integrative Biology, University of California, Berkeley, Berkeley, CA, USA. [3]Department of Ecology and Evolutionary Biology, University of California Santa Cruz, Santa Cruz, CA, USA. [4]University of North Carolina Chapel Hill, Department of Biology, Chapel Hill, North Carolina, USA. [5]Imperiled Species Program, Peninsula Humane Society & SPCA, Saratoga, CA, USA. [6]Department of Fish and Wildlife Conservation, Virginia Polytechnic Institute and State University, VA, USA. [7]Department of Biological Sciences, Ohio Center for Ecological and Evolutionary Studies, Ohio University, Athens, OH, USA. [8]Department of Human Genetics, University of California, Los Angeles, CA, USA. [9]College of Life Sciences, University of Chinese Academy of Sciences, Beijing, China. [10]BGI Research, Wuhan, China. [11]State Key Laboratory of Genome and Multi-omics Technologies, BGI Research, Shenzhen, China. [12]Center of Evolutionary & Organismal Biology, Zhejiang University School of Medicine, Hangzhou, China. [13]Department of Statistics, University of California, Berkeley, Berkeley, CA, USA. [14]Globe Institute, University of Copenhagen, Copenhagen, Denmark. ***Corresponding author. Email: ammoncorl@berkeley.edu** †Deceased.

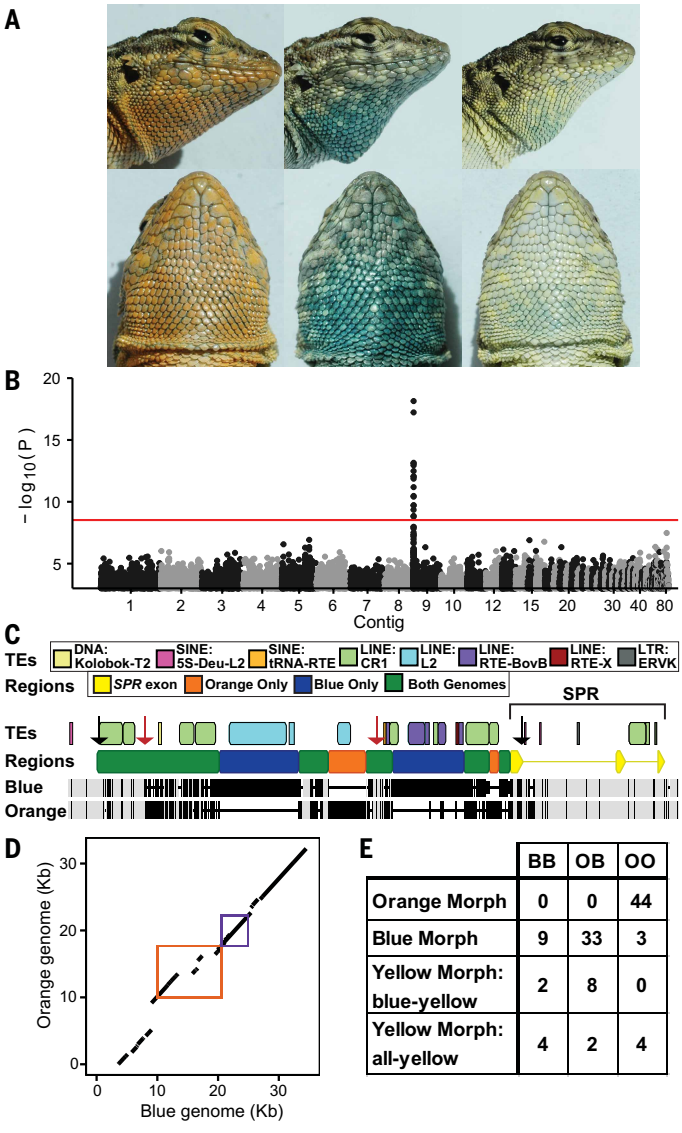

E

	BB	OB	OO
Orange Morph	0	0	44
Blue Morph	9	33	3
Yellow Morph: blue-yellow	2	8	0
Yellow Morph: all-yellow	4	2	4

Fig. 1. Morph phenotypes and associated genetic region. (**A**) (Left to right): Color phenotypes of the orange, blue, and yellow morphs. (**B**) Genetic associations with orange versus blue morph phenotypes. The red line indicates the multiple-testing correction threshold. (**C**) Alignment of the blue and orange morph genomes in the associated region (bottom two rows), showing identical positions (gray), differences (black), and gaps (horizontal lines). The row labeled "Regions" above shows the *SPR* coding region (yellow), alignable sequences between genomes (green), and sequences restricted to the blue genome (blue) and orange genome (orange). The top row shows transposable elements (TEs) colored by the repetitive element family, with the class of TE given before the family name. The arrows indicate top associated positions (red) and primer locations for long-range PCR (black). (**D**) Alignment of the orange and blue morph genomes at the *SPR* coding region (purple) and divergent region upstream of *SPR* (orange). (**E**) Morph genotypes for the O and B haplotype.

High levels of sequence divergence were observed between the two genomes in the associated region upstream of *SPR* (Fig. 1C). Each genome had large regions of sequence not found in the other genome, with most of the genome-specific DNA resulting from the insertion of long interspersed nuclear element (LINE) transposable elements (TEs), primarily L2 and RTE-BovB elements (Fig. 1C). The orange and blue morph genome sequences were colinear at both a broad (fig. S6A) and local (Fig. 1D) level around the region of top association, which showed that the morph phenotypes were not associated with a genetic inversion. The *U. stansburiana* contiguous DNA sequence (contig) with *SPR* was broadly colinear with chromosome 5 of the eastern fence lizard (*Sceloporus undulatus*) (fig. S6B), but little homology was observed to the upstream region in the orange and blue genomes, indicating that both associated regions were highly divergent (fig. S6, C and D).

We further investigated the genetic basis of the color morphs by genotyping 44 orange, 45 blue, and 20 yellow morphs for the two divergent haplotypes observed at the *SPR*-associated region, which we refer to as the orange (O) and blue (B) haplotypes. The genotypes were based on haplotype data obtained from PacBio sequencing of long-range polymerase chain reactions (PCRs) of the *SPR* region and from Illumina short-read data that could establish the presence or absence of the divergent haplotypes. All orange morphs (44/44) had two O haplotypes (OO) whereas blue morphs typically (42/45) had at least one B haplotype (OB or BB, Fig. 1E). The overall pattern suggests a simple genetic basis in which orange morphs are homozygous for the O haplotype and blue morphs have a B haplotype that is dominant to the O haplotype. There were three OO blue morphs, which could indicate a more complex genetic basis, but all blue morphs with photos had a B haplotype, so the anomalous samples could reflect a field categorization error (*29*). Yellow morphs have been categorized as having two different phenotypes (*31*, *37*), with some having all-yellow throats and others having yellow over most of their throats except for a light-blue patch at the base of the throat ("blue-yellow" phenotype, fig. S1C). All blue-yellow males had at least one B haplotype (10/10, Fig. 1E). The majority of all-yellow males had at least one B haplotype (6/10), but some individuals had two O haplotypes (4/10). These OO yellow morphs were smaller than other males (fig. S7), so their yellow coloration could be a transient phase of their color development (*29*). Most yellow morphs have blue-yellow phenotypes (proportion over 23 years of field data = 77% blue-yellow), so if the genotype proportions that we observed are representative (i.e., 100% blue-yellow + 60% all-yellow morphs), this would mean that roughly 91% of yellow morphs have at least one B haplotype. Therefore, the vast majority of yellow morphs have a B haplotype and are genetically similar to blue morphs.

Long-term balancing selection is expected to maintain high levels of genetic diversity. To study this, we first characterized variation among 48 B haplotypes and 108 O haplotypes. There were large regions of haplotype-specific DNA (Fig. 2A), and many additional alignable nucleotides were fixed between haplotypes (Fig. 2B and fig. S8A). Most of these fixed differences were in a region that had high linkage disequilibrium (fig. S8C) and lacked shared polymorphisms between the haplotypes (Fig. 2B), suggesting an absence of recombination between the haplotypes. This nonrecombining region contained the variants with the highest association to morph phenotypes and also TE insertions that were fixed in each haplotype (i.e., all TEs in the blue-only regions and the intervening orange-only region; Figs. 1C and 2A). Levels of nucleotide diversity measured across all haplotypes peaked within and directly adjacent to the nonrecombining region (Fig. 2C), which is consistent with it being under balancing selection. B haplotypes had less genetic variation than O haplotypes, suggestive of a recent selective sweep on the B haplotype. We next compared the nucleotide diversity of the *SPR* region (excluding haplotype-specific DNA) with estimates of nucleotide diversity from across the rest of the genome. The *SPR* region had substantially elevated nucleotide diversity ($\pi = 0.0490$, Fig. 2D) compared with other genomic regions (mean = 0.0046, min = 0.0002, max = 0.0175).

The strong association between morph phenotypes and the upstream region of *SPR* suggests that regulatory changes likely generate morph phenotypes. Therefore, we investigated whether the morphs differed in expression of the *SPR* gene (Fig. 2E and fig. S9) (*29*). The morphs had significant differences in *SPR* expression in colored throat skin [Fig. 2E, coefficient of determination (R^2) = 0.30, $F_{2,21} = 6.0$, $P = 0.0087$]. Blue morphs had higher expression than orange morphs (Fig. 2E, $P = 0.0062$), but

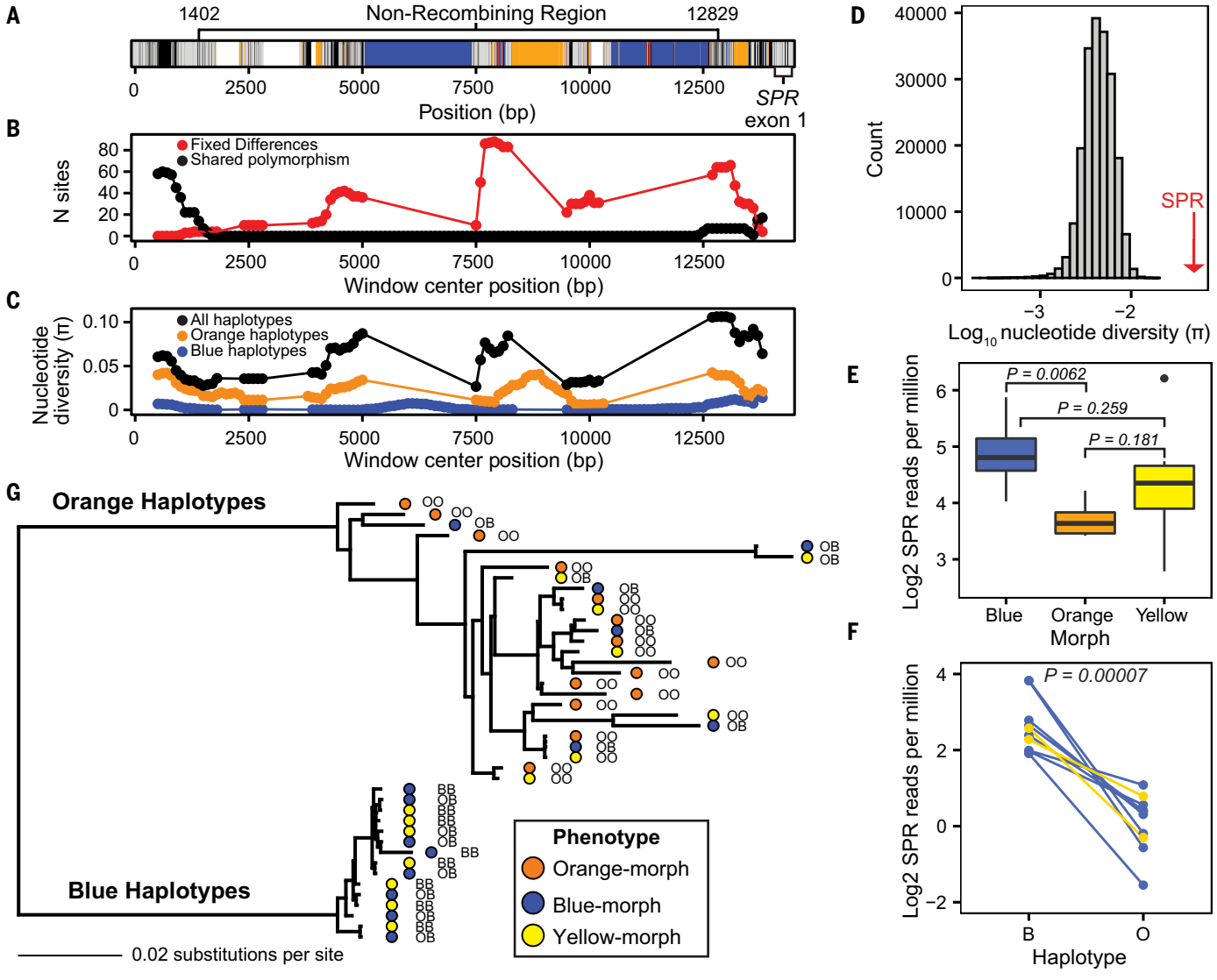

Fig. 2. Genetic diversity, expression, and evolution of the *SPR* region. (**A**) (Top) Overview of the alignment of 48 blue and 108 orange haplotypes showing positions that were invariant (gray), variable (black), primarily gaps (white), exclusive to blue and orange haplotypes (blue and orange), and fixed differences (red). (**B**) The number of fixed differences (red) and shared polymorphic sites (black) between the blue and orange haplotypes. (**C**) Nucleotide diversity (π) for 1000–base pair (bp) windows along blue, orange, and both (black) haplotypes, with gaps as lines. (**D**) Genetic diversity of the *SPR* region (red arrow) relative to other genomic regions. (**E**) *SPR* expression in colored-throat skin. Boxes show the 25th to 75th percentiles with a line for the median, minimum and maximum with whiskers, and a point for an outlier. *P* values indicate post hoc comparisons. (**F**) Haplotype-specific expression in colored skin within individuals heterozygous for the O and B haplotypes. Lines connect the data from an individual, and the colors show blue versus yellow morphs. (**G**) Phylogeny of *SPR*-region haplotypes with associated morph phenotypes (circles) and the *SPR*-region genotype of the individual.

no significant differences were observed in the other two morph comparisons unless a single outlying yellow morph data point was excluded, in which case the difference between blue and yellow morphs was also significant ($P = 0.0221$). *SPR* expression levels were even better explained by a model that took *SPR*-region genotypes into account [fig. S9A; $R^2 = 0.36$, $F_{2,21} = 7.5$, $P = 0.0035$], because the genotypes helped explain variation among yellow morphs, with individuals with a B haplotype having higher expression than OO individuals (e.g., the outlying yellow morph was BB). Compared with orange morphs, blue morphs and individuals with a B haplotype had increased expression of *SPR* in colored skin relative to noncolored skin (fig. S9, C and D), and therefore heightened levels of *SPR* accompany the formation of blue coloration (fig. S5) (*29*). B haplotypes were expressed at higher levels than O haplotypes in individuals heterozygous for both haplotypes (Fig. 2F and fig. S9, E and F, and K). This haplotype-specific expression supports a *cis*-regulatory mechanism (*38*), which is strong evidence that the O and B haplotypes differentially regulate the expression of *SPR*.

We inferred a phylogeny for multiple O and B haplotypes to reveal the evolutionary history of the *SPR* region and to examine whether there were any subtypes of either haplotype that were associated with different phenotypes. The two haplotypes were deeply divergent from each other (Fig. 2G and fig. S10), as expected under long-term balancing selection (*5*). There was no evidence that genetic differences among O haplotypes result in different phenotypes, because the O haplotypes found in heterozygous blue morph individuals and the three anomalous OO blue morphs did not form distinct phylogenetic clusters from O haplotypes in orange morphs. Instead, the blue and orange morphs were only distinguished by the presence or absence of the B haplotype, which is dominant to any O haplotype in generating blue morph

phenotypes. Notably, we also found that the haplotypes from yellow morphs did not form a distinct genetic cluster within either the O or B haplotypes. This observation rejects the hypothesized three-allele model, which requires a third genetic group that differentiates yellow morphs from the other two morphs.

A new model for the genetics of the polymorphism and the development of the yellow morph phenotype was needed. We hypothesized that the yellow morph phenotype arises from developmental phenotypic plasticity, wherein lizards with a B haplotype that are unable to acquire a territory express yellow coloration and adopt a sneaker strategy but express blue coloration if they acquire and defend a territory. This two-allele model with plasticity was supported in several ways (*29*). First, prior field observations and experiments have noted that some yellow morphs can irreversibly transform to a blue morph phenotype late in the breeding season, typically coincident with the opening of a territory (*14*, *21*). Second, blue and yellow morphs have similar *SPR* genotypes (Fig. 1E) and are not distinguished by a distinct type of O or B haplotype (Fig. 2G), and thus both morphs can arise from the same genetic background at *SPR*. Third, yellow morphs could potentially arise from variation at other genes than *SPR*, but genome-wide association tests with yellow morphs failed to reveal any additional candidate genes (fig. S3, C and D), including the *BCO2* gene (fig. S4, C and D) that gives rise to yellow morphs in *P. muralis* (*8*), which makes a multilocus model unlikely. Fourth, we compared the predictions of the two- and three-allele models to 14 years of field surveys of the polymorphism. The two-allele model predicts a positive correlation in the frequency of the blue and yellow morphs within a year because they share the same genetic basis, but it predicts a highly negative correlation between these morphs and orange morphs (Fig. 3A and fig. S11). By contrast, the three-allele model predicts a weak negative correlation among all morphs because an increase in the frequency of one allele necessitates a decrease in the frequency of the other alleles.

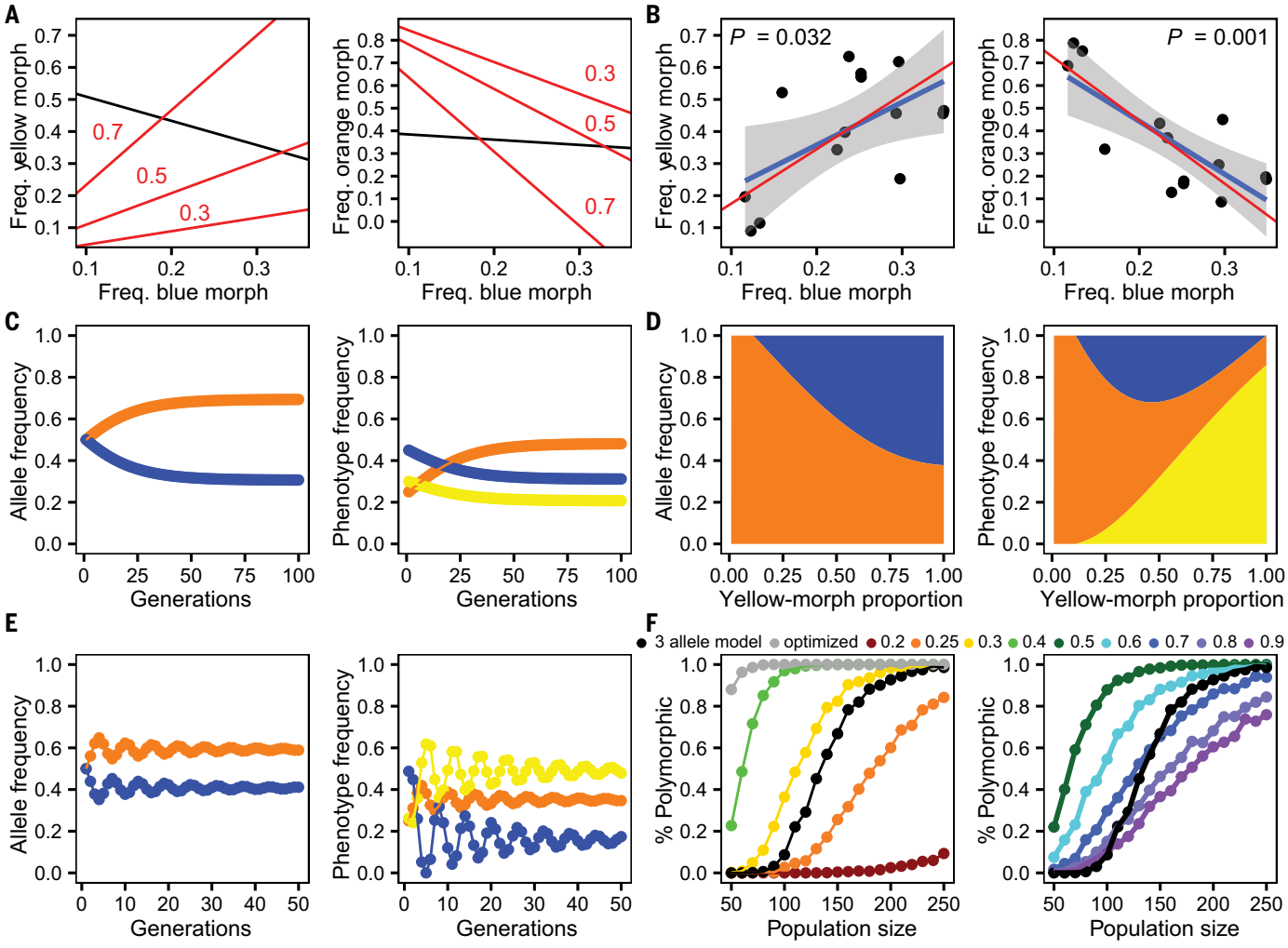

Fig. 3. Morph frequencies, maintenance, and stability. (**A**) Predicted relationships between the frequencies of different morphs from the three-allele model (black line) and two-allele model with different proportions of yellow morphs arising from B haplotype individuals (red lines). (**B**) Correlations in morph frequencies observed in the field data (blue line). The red line is the two-allele model prediction with 64% of B haplotype individuals becoming yellow morphs, as estimated from the field data. (**C**) Simulation using a two-allele model with 40% of B haplotype individuals becoming yellow morphs in each generation. (**D**) The allele and phenotype frequencies observed after 10,000 generations in simulations starting with equal allele frequencies and varying the fixed proportion of yellow morphs in the two-allele model. (**E**) Simulation with a two-allele model in which the proportion of blue and yellow morphs was optimized in each generation but then offset so that 30% more individuals become blue morphs. Morph fitness was estimated from territory-overlap data, whereas other panels used paternity data. (**F**) Stability at different population sizes of the two-allele model with fixed proportions of yellow morphs across generations (colored lines) or optimized within a generation (gray) compared with the three-allele model (black). The *y* axis represents the proportion of 1000 trials in which the polymorphism was maintained for 1000 generations.

The field data clearly matched the predictions of the two-allele model with plasticity because it showed a positive correlation between the frequencies of the blue and yellow morphs (Fig. 3B, $F_{1,12} = 5.92$, $P = 0.032$) and highly negative correlations between the frequencies of these morphs and the frequency of orange morphs (Fig. 3B, $F_{1,12} = 18.10$, $P = 0.001$; and fig. S11).

Our new understanding of the genetics and development of the morphs necessitated a reevaluation of how the mating strategy polymorphism is maintained, because prior studies (*6*, *17*, *19*) used an incorrect genetic model. Our goal was to determine whether rock-paper-scissors fitness dynamics can maintain diversity in a two-allele system, with one allele giving rise to two different phenotypes through irreversible plasticity. We first tested a series of deterministic models with orange morphs arising from homozygotes for the O haplotype, yellow morphs arising from a proportion of all individuals carrying a B haplotype, and blue morphs arising from the remaining individuals with a B haplotype. The parameters of frequency-dependent selection on the morph phenotypes were determined by prior field studies on male territorial interactions and paternity (*6*, *15*, *19*).

The deterministic models showed that two alleles can be maintained by frequency-dependent selection in the form of a rock-paper-scissors game with the plastic generation of two phenotypic strategies (Fig. 3, C to E, and figs. S12 to S14). The two alleles were maintained across a wide range of possible proportions of the yellow sneaker morph, but the system was dominated by the orange allele when the yellow morph proportion was at low values (Fig. 3D and fig. S12), which shows that a minimum proportion of yellow morphs is necessary for the polymorphism to exist. The population genetic models (figs. S12 and S13) and a game theoretical analysis (fig. S15) (*29*) both showed that there are many yellow morph proportions in which a rare orange or rare blue + yellow allele can invade a population of the opposite type and lead to a stably maintained polymorphism. A rock-paper-scissors game based on asexual, fixed strategies exhibits frequency oscillations (*39*, *40*), and morph frequency cycles have been observed in side-blotched lizards (*6*, *19*). Some versions of our two-allele model did exhibit frequency cycles (Fig. 3E and figs. S13H and S14, B and D). The six-generation cycles observed in one version of the two-allele model (Fig. 3E) are more similar to the 5-year cycles observed in nature (*6*, *19*) than the 44-generation cycles of the three-allele model (fig. S14J). Additional factors such as density-dependent selection on the color morphs in females (*41*) or climatic effects on morph frequencies (*17*) could also play a role in generating cycles.

Prior theory suggests that plasticity could affect the stability of a rock-paper-scissors game (*39*, *42*, *43*). We added genetic drift to the models to compare the stability of the two- and three-allele models (Fig. 3F and fig. S16). The two-allele model was more stable than the three-allele model with yellow morph proportions of 30 to 60% for all population sizes and with yellow morph proportions of 70 to 80% for small population sizes (Fig. 3F). A two-allele model that optimized the blue and yellow morph proportions relative to the orange morph frequency had the highest stability. In some cases, there were dramatic differences in stability. At a population size of 100, the three-allele model lost an allele in 91% of the trials, the two-allele model with 40% yellow morphs lost an allele in 3% of the trials, and the optimized two-allele model always maintained the polymorphism. These results show that for a broad range of conditions, the two-allele model with plasticity is superior to the three-allele model at maintaining a genetic polymorphism and that plastic adjustments of morph frequencies within a generation can further promote stability.

Discussion

Our study provides important insights into the genetic basis and evolution of polymorphic phenotypes. First, complex morph phenotypes need not arise from a supergene. Side-blotched lizard morphs do not arise from a chromosomal inversion that links coloration and behavioral genes but instead from variation at a single gene that could couple differences in hormones or neurotransmitters with distinct throat colors through pleiotropy. Although supergenes are a common mechanism for the origin of morphs (*7*, *9*, *10*, *23*), our results and similar observations in other polymorphic species (*11*, *24*) suggest that pleiotropic effects of key regulatory genes are sufficient for generating distinct morph phenotypes. Second, convergent genetic evolution among distantly related species can generate color morphs, as demonstrated by *SPR* being associated with polymorphism in both *U. stansburiana* and *P. muralis* (*8*), which diverged ~179 million years ago (*44*). Studies of birds suggest that morphs often arise from different genes (*7*, *10*, *11*, *23*), but our results and studies of butterflies (*45*, *46*) suggest that certain genes may be repeatedly co-opted to generate color morphs.

Our results also broaden our understanding of how multiple behavioral strategies are maintained within a population. Our models demonstrate that the maintenance of genetic diversity by a rock-paper-scissors game does not require that all the strategies are genetically determined and that the stability of the system is enhanced by having plastic strategies. Phylogeographic study of the side-blotched lizard morphs showed that although the polymorphism has been lost eight times, the color morphs are geographically widespread and have been maintained for millions of years (*5*), which is consistent with the system being highly stable. Examples of rock-paper-scissors dynamics in other species remain rare (*47*–*50*), and theory suggests that three genetically determined strategies will often exhibit unstable dynamics (*51*). However, our findings expand the potential for the rock-paper-scissors game to maintain biodiversity by recognizing that plastic strategies can be part of the game and can promote its stability. There are many species with three male mating strategies that involve a degree of plasticity (*25*–*28*), and the side-blotched lizard polymorphism was initially contrasted to two such species (*52*). We revealed that side-blotched lizard morphs have more in common with species that have plastic strategies than was formerly recognized. Therefore, the maintenance of polymorphism through a rock-paper-scissors game may apply to a much broader array of species than was previously envisioned.

Plasticity could not only help maintain morphs, but it could also facilitate the evolution of biological rock-paper-scissors games. A genetically determined rock-paper-scissors game requires at least two mutations to generate three strategies, but sequential evolution of these mutations would be difficult because only two strategies in a population would be unstable (e.g., the evolution of paper in a population of rock would lead to the loss of rock). This difficulty is removed if two strategies arise from the same genetic background because of plasticity, which might easily occur if behavioral differences accompany morphological changes during development or if there are conditional strategies (*1*, *28*). Plastic strategies can be maintained even with unequal fitness if they are conditionally expressed and increase the fitness of individuals in that condition (*1*, *28*) (e.g., sneaker males may have lower fitness than territorial males, but if a male lacks a territory, sneaking is better than zero fitness). Rock-paper-scissors games could thus evolve either in a plastically dimorphic population if a new mutation generates a third fixed strategy (fig. S12, F and L, and fig. S15) or in a monomorphic population if a new mutation generates two additional strategies through plasticity (fig. S12, D and J, and fig. S15). Thus, plasticity facilitates the simultaneous generation of the three strategies needed for a rock-paper-scissors game, and therefore plastic phenotypes should be integral to many additional biological examples of this game.

REFERENCES AND NOTES

1. M. J. West-Eberhard, *Developmental Plasticity and Evolution* (Oxford Univ. Press, 2003).
2. M. J. West-Eberhard, *Proc. Natl. Acad. Sci. U.S.A.* **83**, 1388–1392 (1986).
3. S. Lamichhaney *et al.*, *Science* **352**, 470–474 (2016).
4. A. Corl *et al.*, *Curr. Biol.* **28**, 2970–2977.e7 (2018).

5. A. Corl, A. R. Davis, S. R. Kuchta, B. Sinervo, *Proc. Natl. Acad. Sci. U.S.A.* **107**, 4254–4259 (2010).
6. B. Sinervo, C. M. Lively, *Nature* **380**, 240–243 (1996).
7. C. Küpper *et al.*, *Nat. Genet.* **48**, 79–83 (2016).
8. P. Andrade *et al.*, *Proc. Natl. Acad. Sci. U.S.A.* **116**, 5633–5642 (2019).
9. M. Joron *et al.*, *Nature* **477**, 203–206 (2011).
10. E. M. Tuttle *et al.*, *Curr. Biol.* **26**, 344–350 (2016).
11. K.-W. Kim *et al.*, *Nat. Commun.* **10**, 1852 (2019).
12. P. Nosil *et al.*, *Sci. Adv.* **10**, eadl3149 (2024).
13. E. I. Svensson, J. Abbott, R. Hardling, *Am. Nat.* **165**, 567–576 (2005).
14. B. Sinervo, D. B. Miles, W. A. Frankino, M. Klukowski, D. F. DeNardo, *Horm. Behav.* **38**, 222–233 (2000).
15. K. R. Zamudio, B. Sinervo, *Proc. Natl. Acad. Sci. U.S.A.* **97**, 14427–14432 (2000).
16. C. Bleay, T. Comendant, B. Sinervo, *Proc. Biol. Sci.* **274**, 2019–2025 (2007).
17. D. Friedman, J. Magnani, D. Paranjpe, B. Sinervo, *PLOS ONE* **12**, e0184052 (2017).
18. R. Calsbeek, S. H. Alonzo, K. Zamudio, B. Sinervo, *Proc. Biol. Sci.* **269**, 157–164 (2002).
19. B. Sinervo, *Genetica* **112-113**, 417–434 (2001).
20. D. C. Haisten, D. Paranjpe, S. Loveridge, B. Sinervo, *Herpetologica* **71**, 125–135 (2015).
21. S. C. Mills *et al.*, *Am. Nat.* **171**, 339–357 (2008).
22. L. D. Ladage, B. J. Riggs, B. Sinervo, V. V. Pravosudov, *Anim. Behav.* **78**, 91–96 (2009).
23. I. Sanchez-Donoso *et al.*, *Curr. Biol.* **32**, 462–469.e6 (2022).
24. A. L. Ducrest, L. Keller, A. Roulin, *Trends Ecol. Evol.* **23**, 502–510 (2008).
25. S. H. Alonzo, M. Taborsky, P. Wirtz, *Evol. Ecol. Res.* **2**, 997–1007 (2000).
26. J. M. Rowland, D. J. Emlen, *Science* **323**, 773–776 (2009).
27. M. Wikelski, S. S. Steiger, B. Gall, K. N. Nelson, *Behav. Ecol.* **16**, 260–268 (2005).
28. M. R. Gross, *Trends Ecol. Evol.* **11**, 92–98 (1996).
29. See the supplementary text in the supplementary materials online.
30. E. I. Svensson, A. G. McAdam, B. Sinervo, *Evolution* **63**, 3124–3135 (2009).
31. B. Sinervo, C. Bleay, C. Adamopoulou, *Evolution* **55**, 2040–2052 (2001).
32. G. Zhang *et al.*, *Proc. Natl. Acad. Sci. U.S.A.* **120**, e2215193120 (2023).
33. J. T. Bagnara, P. J. Fernandez, R. Fujii, *Pigment Cell Res.* **20**, 14–26 (2007).
34. K. Ikemoto *et al.*, *Brain Res.* **954**, 237–246 (2002).
35. E. R. Werner, N. Blau, B. Thöny, *Biochem. J.* **438**, 397–414 (2011).
36. I. Braasch, M. Schartl, J.-N. Volff, *BMC Evol. Biol.* **7**, 74 (2007).
37. B. Sinervo *et al.*, *Proc. Natl. Acad. Sci. U.S.A.* **103**, 7372–7377 (2006).
38. B. Ge *et al.*, *Nat. Genet.* **41**, 1216–1222 (2009).
39. J. Maynard Smith, *Evolution and the Theory of Games* (Cambridge Univ. Press, 1982).
40. A. Szolnoki *et al.*, *J. R. Soc. Interface* **11**, 20140735 (2014).
41. B. Sinervo, E. Svensson, T. Comendant, *Nature* **406**, 985–988 (2000).
42. M. Kleshnina, S. S. Streipert, J. A. Filar, K. Chatterjee, *PLOS Comput. Biol.* **17**, e1008523 (2021).
43. S. Moulherat *et al.*, *Sci. Rep.* **7**, 15939 (2017).
44. F. T. Burbrink *et al.*, *Syst. Biol.* **69**, 502–520 (2020).
45. R. D. Reed *et al.*, *Science* **333**, 1137–1141 (2011).
46. N. J. Nadeau *et al.*, *Nature* **534**, 106–110 (2016).
47. B. Kerr, M. A. Riley, M. W. Feldman, B. J. M. Bohannan, *Nature* **418**, 171–174 (2002).
48. B. Sinervo *et al.*, *Am. Nat.* **170**, 663–680 (2007).
49. B. Sinervo, R. Calsbeek, *Annu. Rev. Ecol. Evol. Syst.* **37**, 581–610 (2006).
50. D. Semmann, H.-J. Krambeck, M. Milinski, *Nature* **425**, 390–393 (2003).
51. S. H. Alonzo, R. Calsbeek, *J. Evol. Biol.* **23**, 2614–2624 (2010).
52. J. M. Smith, *Nature* **380**, 198–199 (1996).
53. A. Corl *et al.*, Data from the paper: The genetics, evolution, and maintenance of a biological rock-paper-scissors game, Dryad (2025); https://datadryad.org/dataset/doi:10.5061/dryad.4qrfj6qq7.

ACKNOWLEDGMENTS

Thanks to the Arbelbide family for permission to work on their land. Thanks to Pacific Biosciences, N. Bittner, B. Karin, O. Nguyen, B. Bach, and X. Valencia for help with PacBio sequencing. Thanks to two anonymous reviewers for helpful comments that improved the paper. **Funding:** This work was supported by NSF grants EF1241848 (B.S., D.B.M.) and DEB1950636 (D.B.M.) and NIH grant R35GM153400 (R.N.). **Author contributions:** A.C., P.B., R.S., R.C., D.M., J.A.M, R.C.K.B, and B.S. contributed to fieldwork; A.C., J.M.V., P.H.S., J.G., X.X., Y.Z., Q.L., and G.Z. performed lab work and analyses related to genome assembly; A.C., A.Gu., L.S., and K.B. performed other lab work; A.C., K.B., A.Go., and R.N. analyzed the data; A.C. and R.N. performed the modeling; A.C. and R.N. wrote the first draft of the paper, which was edited by the other authors. **Competing interests:** The authors declare that they have no competing interests. **Data, code, and materials availability:** The genetic data from this study has been deposited in the Sequence Read Archive in BioProject PRJNA1328718 and in GenBank (accession numbers PX436996 to PX437172 and PX512685 to PX512686). Additional data and the R-code used to analyze the data are available on Dryad (*53*). The specimens underlying the genetic work have been deposited in the Museum of Vertebrate Zoology at the University of California, Berkeley. The museum catalog numbers and the genetic accession numbers for all samples are available on Dryad in the following files: Uta_DNAseq_samples_with_SRA_accession_numbers.xlsx, Uta_RNAseq_samples_with_SRA_accession_numbers.xlsx, and Uta_PacBio_amplicon_metadata_and_Genbank_ID.xlsx.

SUPPLEMENTARY MATERIALS

science.org/doi/10.1126/science.adw8265
Materials and Methods; Supplementary Text; Figs. S1 to S16; References (*54*–*116*); MDAR Reproducibility Checklist

Submitted 25 February 2025; accepted 27 October 2025

10.1126/science.adw8265

The genetics, evolution, and maintenance of a biological rock-paper-scissors game

Ammon Corl, Alex Guzman, Ke Bi, Juan Manual Vazquez, Lydia L. Smith, Pauline Blaimont, Regina Spranger, Robert D. Cooper, Donald Miles, Amy Goldberg, Jian Gao, Xueyan Xiang, Yang Zhou, Qiye Li, Guojie Zhang, Peter H. Sudmant, Rauri C. K. Bowie, Jimmy A. McGuire, Barry Sinervo, and Rasmus Nielsen

Science **391** (6780), . DOI: 10.1126/science.adw8265

Editor's summary

Many animal species exhibit different physical characteristics between individuals, especially when it comes to males. Lizards are particularly interesting examples, because many species have multiple versions of males. Studying these species can inform understanding of how such polymorphism evolves and operates. Uller *et al*. found that a recently emerged white throated morph of European wall lizards was highly preferred over an earlier three-color system, which has led to disruption of a million-year balance across the morphs (see the Perspective by Gopalan and Castoe). In related work on side-blotched lizards in the United States, Corl *et al*. found that a well-known morphological triad of males was generated by a two-allele system, with phenotypic plasticity at one of the alleles and a rock-paper-scissors dynamic. —Sacha Vignieri